JMEPEG (2010) 19:685–692
DOI: 10.1007/s11665-009-9543-2

1059-9495/$19.00

The Influence of Calcite, Fluorite, and Rutile on the Fusion-Related Behavior of Metal Cored Coated Electrodes for Hardfacing

Amado Cruz-Crespo, Rafael Fernández Fuentes, and Américo Scotti

(Submitted December 20, 2008; in revised form July 25, 2009)

Coated electrodes for SMAW have exhibited their advantages for longer than one century. Means of boosting their performance, particularly for hardfacing, would be a raise in the alloying transfer efficiency and a lowering of the dilution with the substrate, without losing the production capacity. In this study, an evaluation about the operational behavior of a new conception of electrodes for hardfacing is described, i.e., metal cored coated electrodes. Experimental electrodes were produced using metal cored technique to obtain the rods. FeCrMn was used as alloying material at two grain sizes. Using the Mc Lean Anderson experimental design approach, the content ratio of $CaCO_3$:CaF_2:TiO_2 in the coating was varied. The effect of the coating composition and granulometry of the filling alloying material on the formation a cannon-like end was assessed. Fusion and metal transfer behaviors were evaluated through measurements of fusion and deposition rates, deposition efficiency, and duration and frequencies of short-circuiting. Based on a balance of performances, the most appropriate composition for the coating was determined. It was also observed that a coarser FeCrMn presented better performance.

Keywords coated electrodes, fusion and deposition rates, hardfacing, metal cored, metal transfer, SMAW, welding

1. Introduction

The extended and endless application lifetime of the SMAW process is related to its metallurgical and operational versatility, allied to its relatively low costs. The coating importance in the SMAW electrode performance is well known and several researchers have recognized the complexity involved in the design of new coatings (Ref 1-10). This subject is still relevant, despite the fact that it has been systematically studied for a long time, as exampled by Vornovitskii and Vagarov's (Ref 11) and Pokhodnya et al.'s (Ref 12) work. Naturally, the interest on this matter in not exclusively scientific, yet a deep knowledge on its physical and metallurgical aspects have arisen from fundamental studies (such as metal and electrical charge transfer, fusion and heat-affected zone microstructure, alloying elements pick-up, slag properties, etc.). Semendyaev (Ref 13) wrote an article with more commercial emphasis, while Surian's (Ref 14) and Yarovchuk et al.'s (Ref 15) emphases were more on operational behavior, yet always with the intention of either increasing the range of applied raw materials used in the electrode manufacturing or improving the quality and efficiency of them, looking for more flexible market strategies. If on one hand, the majority of manufactures sustain the production quality based on the fusion-related parameters, as pointed out by Semendyaev (Ref 13) and Sulima and Kucherova (Ref 6) and, evidently, in the deposited metal proprieties, as defined in the electrodes datasheets, on the other hand there are a few researches concentrated on more phenomenological approaches (metal and alloy element transfers, weld metal, heat-affected zone micrographs, slag role, etc.), as found evidences in the papers delivered by Scotti et al. (Ref 16), Vornovitsky et al. (Ref 8), Mazel (Ref 5), Yarovchuk (Ref 10), and Farias et al. (Ref 4).

From one side to other, the searches for better ($>60\%$) coated electrode efficiencies (economically or properties related) take into account the coating composition. However, most pieces of work, as seen in the referred paper titles, deals with a linear effect of a component, yet conditioned to others. In a study on the effect of the Mg on the arc stability, Farias et al. (Ref 3) observed that slag properties changed concomitantly. Sometimes, researchers could not explain the results, as reported by Yarovchuk (Ref 10). He concluded that the concepts of basicity and relative chemical activity are not totally applied to explain the thermodynamic system of slag with high TiO_2 and SiO_2 contents.

In a previous study, Cruz-Crespo et al. (Ref 17) showed to be possible to make novel developments on coated electrodes; tubular-coated electrodes for hardfacing were developed with different inner ferroalloy grain sizes, and, comparatively to a conventional commercial coated electrode, welded at a range of setting currents. In the same directions, other authors (Ref 18-20) have investigated this approach for SMAW, and even commercial products have been reported (STOODY-31, presented at the STOODY Product Selection Guide: Build-Up

Amado Cruz-Crespo and **Rafael Fernández Fuentes**, Center for Welding Researches, Universidad Central "Marta Abreu" de Las Villas, Carretera a Camajuaní km 5.5 Villa Clara, Santa Clara, Cuba; and **Américo Scotti**, Center for Research and Development of Welding Processes, Universidade Federal de Uberlândia, Campus Santa Mônica, 30400-902 Uberlândia, MG, Brazil. Contact e-mails: acruz@uclv.edu.cu, rfernandez@uclv.edu.cu, ascotti@ufu.br, and ascotti@mecanica.ufu.br

and Hardfacing Electrodes and Wires, Form No 2102A). All the cited sources are concerning hardfacing, but only Cruz-Crespo et al.'s study (Ref 17) also focussed the operational behavior of consumables (e.g., short-circuit frequency, short-circuit duration, fusion, deposition rate, etc.). In this latter referred work, the authors found a current range for each of the electrode conceptions in which the operational behavior (bead penetration and dilution, geometry, deposition rate and efficiency, etc.) is particular and optimized. They also observed that even the alloying element size in the electrode core affects this current range. They concluded that the current ranges for the tubular electrodes are narrower than for a conventional electrode of same application. They finally found that the dilutions between filler and parent metals with metal cored coated electrode are lower than with conventional coated electrode, important characteristic for hardfacing operation (less loss of alloying elements). However, there is still a fabrication cost limitation for the tubular electrodes.

However, in those papers the importance of the coating composition has not been discussed. So, this study was designed to study the effect of calcite, fluorite, and rutile on the fusion-related behavior of those metal cored coated electrodes for SMAW hardfacing.

2. Materials and Methods

The tubular electrodes are composed of a plain carbon metal tube, a filling material, and a coating material. In this study, the filling material was essentially ferroalloying compounds (FeCrMn), while the coating provided the arc stabilizers, deoxiders, and slag/gas formers. Two types of experimental tubular electrodes used were: (i) denominated CIS-C (standing to coarse), in which the granulometry of the ferroalloying ranged from 0.1 to 0.25 mm and (ii) denominated CIS-F (standing to fine), with the alloying component grains $\leq$0.1 mm. The ferroalloys filled with a 4-mm-diameter (external), 350-mm-long tube. The alloying load and the tubular electrodes were obtained as described by Cruz-Crespo et al. (Ref 18) in a previous work. On each type of tubular electrodes, coatings (basic) were employed with systematic variations of calcite ($21\% \leq X_1 \leq 57\%$), fluorite ($21\% \leq X_2 \leq 57\%$), and rutile ($0\% \leq X_1 \leq 57\%$), totaling 100% in a triangular composition.

The coating formulations took the same composition of a previously used tubular-coated electrode as a starting criterion (Ref 17, 18), in which the ratio calcite/fluorite was equal to 1 and no rutile was joined to them. Therefore, this study looked for evaluating a wide range of calcite and fluorite around this initial point, under the influence of rutile (from 0%) too. The definition of the contents of each component (factors) was based on a statistical design of experiments (Mc Lean Anderson) for restrained regions (Ref 21). Only 6 out of 12 possible combinations ($N = q \times 2^{q-1}$, where N is the demanded number of experiments and q is the number of independent factors) accomplished with the condition of normalization ($\sum X_i = 100\%$) and not presented factors values outside the defined range. Figure 1 illustrates the experimental design inside the triangular diagram, pointing out the six vertices that represented the combination of each coating formulation. A seventh combination was defined at the center of the operational envelop.

The coating was manufactured from minerals rich in each of the main ingredients, 98.6% of $CaCO_3$, 96.1% of CaF_2, and 99.0% of TiO_2, respectively, for calcite, fluorite, and rutile. Such minerals' characteristics had been reported elsewhere (Ref 22, 23). To each mixture, 10% of graphite was added to the summation of calcite, fluorite, and rutile. Before mixing all components, each one was grounded to a size of $\leq$0.1 mm, by using a mill and mesh sieves, which were weighed in a 0.1 g resolution lab scale and homogenized (entering by density crescent order) in a rotational barrel during 30 min. To the dry mixture, sodium silicate (29.39% SiO_2, 10.10% Na_2O, and 60.51% H_2O) was added at a ratio of 4:10 in weight (silicate/mixture). A paste consistency was reached by complementary water. Then, the coating was manufactured by the immersion of the tubular rods into the paste. Seven groups of electrodes with ferroalloying in the core ranking from 0.1 to 0.25 mm and seven other groups with the alloying granulometry $\leq$0.1 mm were obtained. Finally, theses electrodes were baked at 160 °C × 2 h.

Bead-on-plate welds were carried out on AISI 1020 plates of $200 \times 30 \times 9.2$ mm^3 in the flat position. To eliminate the skill influence of the welder, the welds were deposited by using an automatic voltage control system, which keeps the desired arc length constant along the electrode fusion (Ref 24). The arc was kept as short as a welder does, by setting the reference voltage (U_{Ref}) at 25 V, even though some small differences in arc length among the electrodes may be expected, since they have different composition. The travel speed was set at 10 cm/min. An average current of 120 A (DCEP) was defined by making use of a previous paper (Ref 19). The electrodes were positioned in an angle of −15° (pushing) in relation to the welding direction.

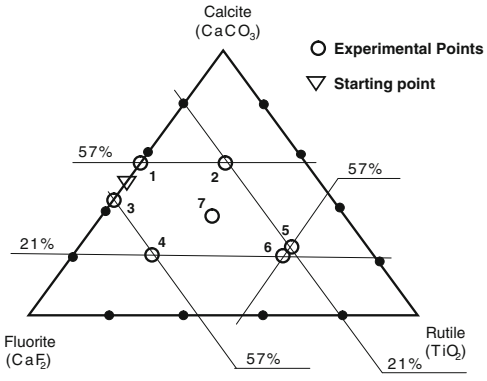

Fig. 1 Design of the experiments

Batch	Calcite (%)	Fluorite (%)	Rutile (%)
1	57	43	0
2	57	21	22
3	43	57	0
4	21	57	22
5	22	21	57
6	21	22	57
7(C)	37	37	26

The test plates and the electrodes (or remaining parts of them) were individually weighed before and after welding, so that the deposited and consumed mass of the electrodes could be determined. Current and voltage signals were recorded at a rate of 10 kHz, 12 bit of resolution, during 6 s. A dedicate computer program was used to treat the recorded instantaneous values so that metal transfer related information could be quantified (number and frequency of short-circuits and short-circuit durations). With these quantities, regression analysis modeling was obtained to establish the dependence of them with the coating composition (calcite, X_1; fluorite, X_2; and rutile X_3). Eventually, response surface plots were drawn using the commercial software Statgraphic® to illustrate the referred dependences.

3. Results and Discussions

3.1 Relationship Between Cannon Effect and Coating Composition

Cannon effect is a coating-related behavior of coated electrodes that makes the metallic core to burn in advance in relation to the coating, so that the electrode end takes a cannon shape. The size of the cannon depends on the coating composition and current level. This cannon effect plays an important role in the coated electrode performance, since the shape taken by the coating directs the droplets under transfer straight to the plate, governing their growing and preventing spattering.

It is impossible to determine the actual length of the cannon in the electrode end during welding, but a good approximation is possible by measuring the depth of the core end inside the coating cannon after arc extinguishing. The resulting mean values of the cannon (cannon effect or CE) are shown in Table 1 as a function of the ratio between the external diameters of the coating and the metallic core, called coating factor (CF). The coating basicity (CB) index is also presented in this table, determined by means of application of an expression presented by Podgayetskii and Kuzmenko (Ref 25), which considers the mass molar relationship among the coating components. For calculating the basicity, the chemical composition of the slag was estimated by considering the composition of the minerals that take part in the coating formulation and the transformation that they experiment during the pyrometallurgic treatment, as mentioned before by Cruz-Crespo et al. (Ref 23).

It is important to point out that, due to the manufacturing method for coatings (immersion), CF cannot be considered here as a variable, despite the deviation of the mean values of each experimental electrode. It is statistically reasonable to take as figure the mean value among the 7 runs (1.6 ± 0.1 for both CIS-C and CIS-F, confirmed by the hypothesis test of equality, at 95% of confidence, which shows no significant differences between the means, i.e., $F_{calculated}$ for CIS-C = 1.63 and $F_{calculated}$ for CIS-F = 1.58 are smaller than $F(0.5,6,6.63) = 2.18$). On the other hand, as CB is related to the coating formulation, its value varied significantly for each run, yet no regular relation between CB and CE was possible to be reached. However, by processing the effects of calcite, fluorite, and rutile contents in the coatings (Fig. 1) over the cannon formation, plots shown in Fig. 2 and 3 became possible to be obtained. A higher CB means more pronounced cannon effect. In other words, a negative value for CE means that the coating composition would favor the fusion of the coating end in advance in relation to the metallic core. This is an extrapolation of the results, since no coating combination in the experiments reached a negative CE.

A tendency of increasing the cannon size for higher content of calcite and a lower content of fluorite was observed. This finding disagrees with De Rissone et al. (Ref 2), who showed a contrary tendency for calcite. However, in De Rissone et al.'s work, the variation of calcite composition was in a lower percentage, in addition to a parallel variation in the contents of SiO_2 and cellulose. In contrast, Brandi et al. (Ref 26) demonstrated somehow concordant results, since the cannon effect was stronger for a basic electrode (AWS E7018). Rutile seems to play a minor role.

Table 1 Coating characteristics (Coating—CF and Basicity—CB factors) and respective resultant cannon effect (CE)

	CIS-C			CIS-F		
Batch	CF	CB	CE, mm	CF	CB	CE, mm
1	1.7	2.82	2.1	1.8	2.82	2.2
2	1.7	2.19	5.7	1.8	2.19	5.7
3	1.8	2.43	1.7	1.7	2.43	1.6
4	1.5	1.37	0	1.6	1.37	0
5	1.5	0.87	1.2	1.5	0.87	2.2
6	1.6	0.85	1.2	1.5	0.85	2.5
7 (C)	1.5	1.65	0.3	1.5	1.65	0.6

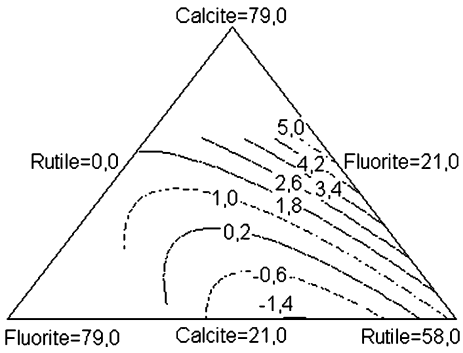

Fig. 2 Cannon effect (mm) as a function of calcite, fluorite and rutile contents for the CIS-C electrodes

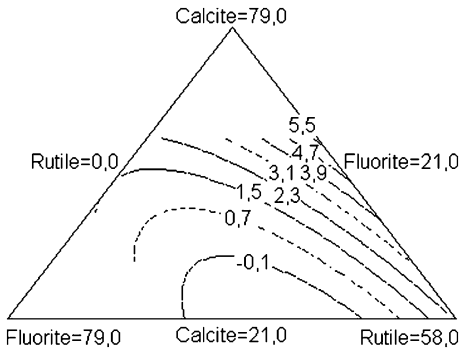

Fig. 3 Cannon effect (mm) as a function of calcite, fluorite and rutile contents for the CIS-F electrodes

The positive effect of calcite on the formation of the cannon might be connected to a higher fusion temperate reached by the coating when calcite content is high. By the same reasoning, a reducing cannon effect would be expected from higher content of fluorite (which makes the fusion temperature to decrease; Ref 23, 25). However, one must remember that an independent analysis of each component is not possible, since other coating component contents vary simultaneously. Thus, as mentioned by Podgayetskii and Kuzmenko (Ref 25), a component acts according to its interactions in the equilibrium system, which could be interpreted as changes in the liquidus line position in relation to pure components. The similarity between the maps of Fig. 2 and 3 indicates that granulometry of the ferroalloying does not play an important role on the cannon formation.

3.2 Relationship Between Fusion and Deposition Rates and Coating Composition

Figures 4 and 5 show the expected effects of the coating composition on the fusion rate for both electrode types. In both cases, the electrodes melt faster if fluorite is increased. The reason may rely on the characteristic of fluorite of reducing the fusion temperature of the component mixture (Ref 23, 25). On the other hand, at least for this three-part system, the contents of calcite and rutile seem to not change the fusion behavior of the electrodes.

At first view of the comparison between Fig. 4 and 5, one could point out an effect of the grain sizes of the ferroalloyings (CIS-C has coarser filling), since the isoline map for the electrode CIS-F presents a maximum region at the center. However, considering the number of experiments, the differences are not statistically relevant, either concerning the tendencies or considering the values (the fusion rate increased in both cases from around 22 g/min to around 30 g/min when fluorite is increased in the mixture from 21% to around 70%).

However, fusion rate is not a comprehensive parameter for evaluating the performance of an electrode, since it does not reflect the amount of material deposited. Deposition rate would be the parameter that is production related (time and cost). A part of the electrode (coating, tubular rod, and ferroalloying filling) that is fused is not converted into weld bead. Apart from spattering, the coating, in special, is generator of slag and fumes. However, as seen in Fig. 6 and 7, the effect of the coating composition on deposition rate is very similar to on fusion rate, that is, the deposition rate increases as fluorite content gets higher in the mixture. Calcite and rutile do not play important role in the phenomenon.

Regardless the importance of the parameter deposition rate, the deposition efficiency is the one which gives us a better idea on how much material loses during welding. Figures 8 and 9 present the isoline maps of the deposition efficiency tendencies for both electrodes. It is interesting to notice that, despite the fact that an increasing fluorite content favor higher fusion and deposition rates, the effect on deposition efficiency is the opposite (at low fluorite, the deposition efficiency increases from around 60% to approximately 65%). It is important to recall that the loss of material which determines the deposition efficiency can be divided into two classes. The first one is

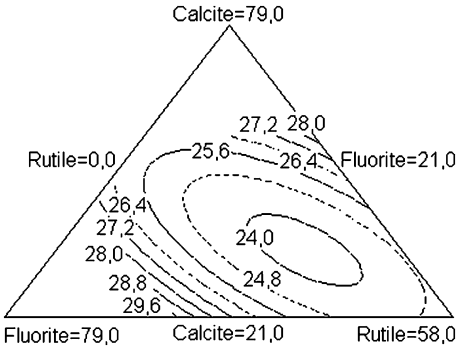

Fig. 4 Fusion rate (g/min) at 120 A as a function of calcite, fluorite, and rutile contents for the CIS-C electrodes

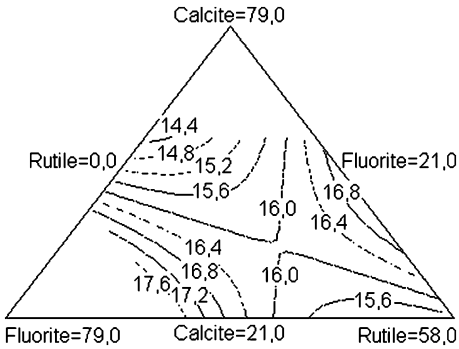

Fig. 6 Deposition rate (g/min) at 120 A as a function of calcite, fluorite, and rutile contents for the CIS-C electrodes

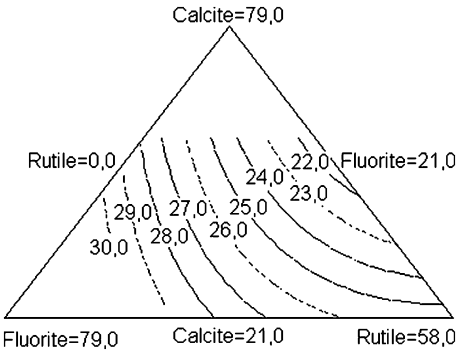

Fig. 5 Fusion rate (g/min) at 120 A as a function of calcite, fluorite, and rutile contents for the CIS-F electrodes

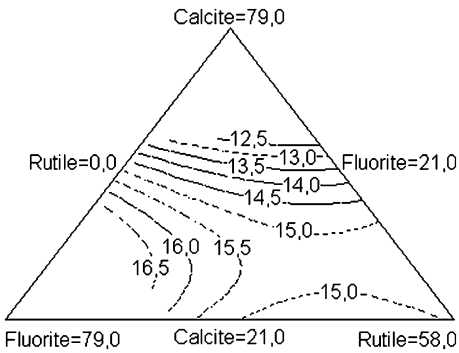

Fig. 7 Deposition rate (g/min) at 120 A as a function of calcite, fluorite, and rutile contents for the CIS-F electrodes

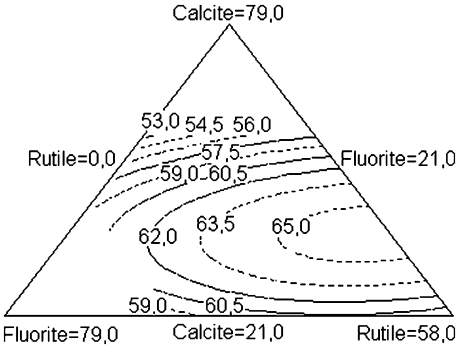

Fig. 8 Deposition efficiency (%) at 120 A as a function of calcite, fluorite, and rutile contents for the CIS-C electrodes

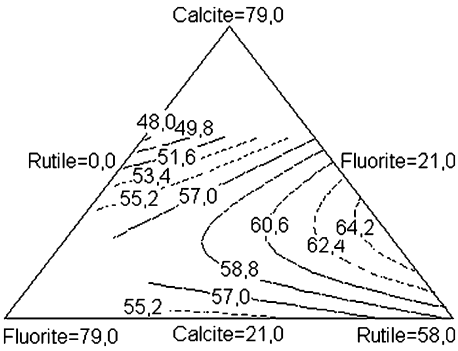

Fig. 9 Deposition efficiency (%) at 120 A as a function of calcite, fluorite, and rutile contents for the CIS-F electrodes

related to metal loss by means of spattering. The second one is related to decomposition of the coating and alloying filling during arcing, converting into slag and fumes. However, the metallurgical reaction between the coating and filling with the fused metal can either introduce mass to the weld pool (aggregating metallic elements, as expected from the ferro-alloyings) or remove mass (picking up elements toward slag and fumes).

In relation to the first class, it would be easy to explain the increase in the deposition efficiency as fluorite is reduced in the coating composition, since one can expect that the cannon effect would reduce spattering (the cannon behavior gets stronger to lower fluorite contents). But some metallurgical reactions could justify an offset effect, as detailed in Table 2. From the elements present in the coating, rutile, fluorite, and sodium silicate are transferred straight to the slag. Calcite, in turn, goes through a dissociation process at relatively low temperature, releasing CO_2 and imputing CaO to the slag. The graphite presented in the coating can partially oxidize, changing into gas, but a part is transferred to the weld pool as carbon (important to the type of electrode). Thus, material from the electrode is lost as slag and fumes/gases.

Podgayetskii and Kuzmenko (Ref 25) narrate that fluorite increases the basicity, favoring the transfer of alloying elements, such as Cr and Mn, to the pool. In turn, the content of CaF_2 brings on a double effect. From one side, a part of the anions F^- replaces with relatively facility the anions O^{2-}, due to its similarity in atomic size (1.33 Å for F^- and 1.36 Å for O^{2-}), breaking the liaison Si-O and forming volatiles fluorites

Table 2 Main reactions that happens during welding, justifying the losses of mass as slag and fumes and transfer of metallic elements to and from the weld pool

In the coating	In the slag
$CaCO_{3coating} = (CaO) + \{CO_2\}$	$2(CaF_2) + (SiO_2) = 2(CaO) + \{SiF_4\}$
$C_{coating} + \{O_2\} = \{CO_2\}$	$(CaO) + (SiO_2) = (CaSiO_3)$
$C_{coating} + 1/2\{O_2\} = \{CO\}$	$(CaO) + (TiO_2) = (CaTiO_3)$
	$2(CaF_2) + (SiO_2) = 2(CaO) + \{SiF_4\}$
In the weld pool	**In the interface slag-weld pool**
$[C] + [FeO] = [Fe] + \{CO\}$	$2(MnO) + [Si] = 2[Mn] + (SiO_2)$
$[Mn] + [FeO] = [Fe] + (MnO)$	$2(Cr_2O_3) + 3[Si] = 4[Cr] + 3(SiO_2)$
$[Si] + 2[FeO] = 2[Fe] + (SiO_2)$	$(MnO) + [C] = [Mn] + \{CO\}$
$2[Cr] + 3[FeO] = 3[Fe] + (Cr_2O_3)$	$(Cr_2O_3) + 3[C] = 2[Cr] + 3\{CO\}$
	$(Cr_2O_3) + 3[Mn] = 2[Cr] + 3(MnO)$
	$2[Fe_2P] + 5[FeO] + 4(CaO) = (CaO)_4P_2O_5 + 9[Fe]$
	$[FeS] + (CaO) = (CaS) + [FeO]$
	$3(CaF_2) + 4[FeS] = 3(CaS) + \{SF_6\} + 4[Fe]$

(..) = Present in the slag; […] present in the weld pool; and {..} present in the fumes

with Si and, consequently, reducing SiO_2 in the system. From the other side, the cations of Ca^{2+}, introduced by the CaF_2, are allocated in the voids originated by the Si-O liaison breakage, shrinking the chemical siloxane bridges (-Si-O-Si-O-Si- + $CaF_2 \rightarrow$ -Si-O-Ca^{2+}-O-Si-F + F-Si-) and, consequently making the slag more fluid. Concerning the effect of Ti, Podgayetskii and Kuzmenko explain that, on the one hand, TiO_2 reduces the basicity of a system (it appears in the denominator of the basicity equations) and metallic element transfer to the pool should be weakened. However, on the other hand, according to Yarovchuk (Ref 10), an increase in TiO_2 can after its dissociation to chemically reduce SiO_2 to Si (now, the system basicity gets higher). As a result, more Si is transferred to the pool, minimizing the loss of Cr and Mn by oxidation.

3.3 Influence of the Coating Composition on the Metal Transfer

For coating electrodes, one can consider that the droplet is transferred to the pool in a short-circuiting mode (governed by surface tension and detached though a instantaneous short-circuit peak current) when the short-circuit takes 2 ms or longer. Shorter short-circuits are considered incipient and no transfer takes place. A very long short-circuit duration means operational instability. And, an electrode is considered stable from the metal transfer point of view if the average short-circuiting duration is closer to 3-4 ms and its standard deviation is as minimal as possible. These data together with the number of these short-circuits per unit of time (or the frequency rate) make possible the estimation of the average masses and sizes of the drop under transfer [it is not considering here the volume of slag covering the drops under transfer, as described by Brandi et al. (Ref 26)]. Table 3 quantifies the effect of the coating

Table 3 Resultant average values of short-circuiting frequency (Fsc) and duration (tsc) and estimated values of drop mass (M_d) and diameter (D_d) as a function of the electrode coating composition for electrodes CIS-C and CIS-F (it is considered that all metal transfers happened only in short-circuiting mode with duration ≥2 ms)

	CIS-C				CIS-F			
Batch	Fsc, Hz	tsc, s	M_d, g	D_d, mm	Fsc, Hz	tsc, s	M_d, g	D_d, mm
1	4.0	0.0067	0.0594	1.2	7.5	0.0051	0.0294	1.0
2	3.5	0.0052	0.0792	1.3	2.5	0.0051	0.0815	1.4
3	7.7	0.0099	0.0363	1.0	15.3	0.0067	0.0183	0.8
4	7.2	0.0210	0.0416	1.1	8.2	0.0074	0.0321	1.0
5	2.3	0.0070	0.1129	1.5	8.2	0.0148	0.0306	1.0
6	3.5	0.0090	0.0730	1.3	11.5	0.0056	0.0221	0.9
7(C)	4.5	0.0124	0.0592	1.2	8.0	0.0045	0.0316	1.0

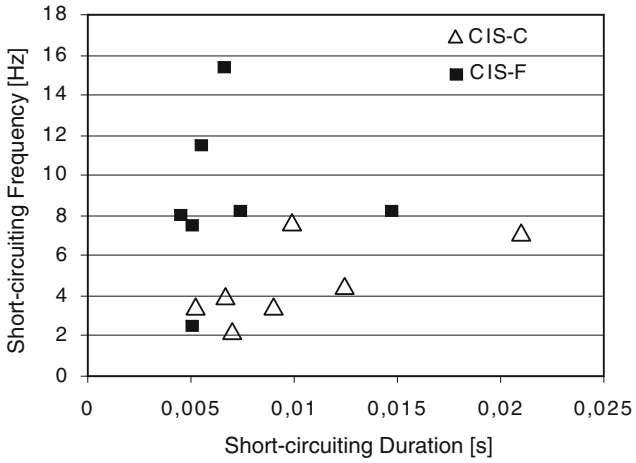

Fig. 10 The relationship between short-circuiting duration and frequency as established in Table 3

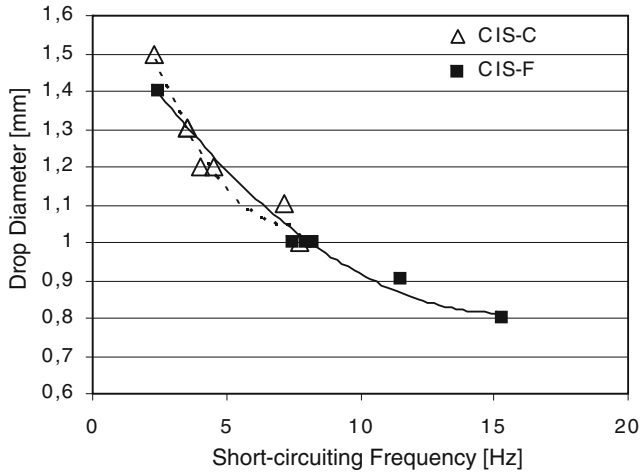

Fig. 11 Relationship between the measured short-circuiting frequency (Fsc) and calculated drop diameter (D_d) for the electrodes CIS-C and CIS-F

composition on the metal transfer short-circuiting characteristics of the two types of electrodes.

One could expect that the longer the short-circuiting duration time (tsc) the lower the short-circuiting frequency (Fsc). However, one droplet, due to the composition of the system metal-slag, can take, for instance, long time transferring (tsc), yet, due to its the fusion characteristics, a short time between the drop formation and the contact drop-pool (time which is called arcing time). Thus, there is no straight relationship between tsc and Fsc, as seen in Fig. 10. On the other hand, Fig. 11 shows another characteristic taken from Table 3, using the drop diameter (D_d) calculations. As expected, the higher the short-circuiting frequency, the smaller the drops under transfer. But, the electrodes CIS-C (coarser alloying filling) are prone to larger drops and lower frequency.

Figures 12-15 illustrate the influence of the coating composition contents on the metal transfer characteristics. The shapes of the isolines are very similar, but the figures that each isoline represents are quite different. It means that the coating composition presented a characteristic effect on the metal transfer behavior, but there is also a strong influence of the granulometry of the filling alloying compounds. From these isoline plots, it is clear that an increase of the fluorite contents makes "Fsc" bigger, but the coarser alloying filling (CIS-C) presents lower frequencies. Concerning "tsc," on the other hand, the most important component is calcite: the lower the

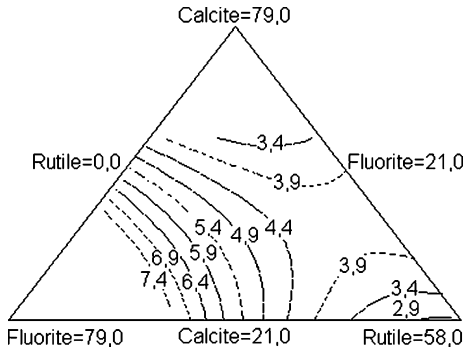

Fig. 12 Short-circuit frequency (Hz) at 120 A (only tsc ≥ 2 ms) as a function of calcite, fluorite, and rutile contents for the CIS-C electrodes

calcite content the longer the "tsc". Similarly, the granulometry of the filling alloying compounds affects this characteristic: coarser alloying filling (CIS-C) presents longer transferring time.

As seen in Fig. 4 and 5, both electrode types melt faster if fluorite is increased. This gives explanation for a higher frequency needed to keep the process stable. However, the

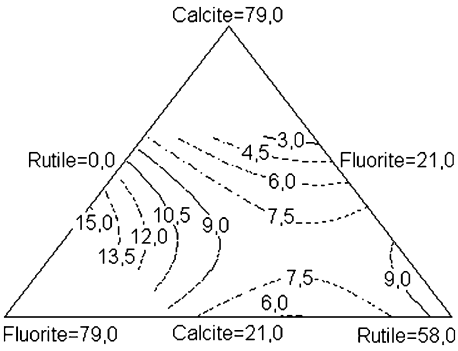

Fig. 13 Short-circuit frequency (Hz) at 120 A (only tsc ≥ 2 ms) as a function of calcite, fluorite, and rutile contents for the CIS-F electrodes

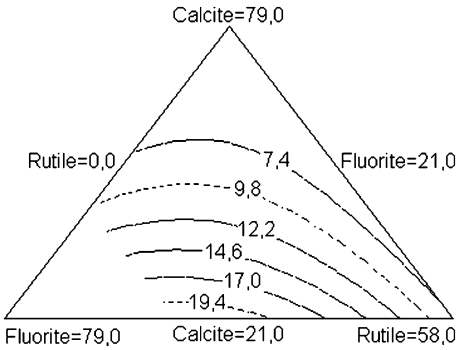

Fig. 14 Short-circuit duration (ms) at 120 A (only tsc ≥ 2 ms) as a function of calcite, fluorite, and rutile contents for the CIS-C electrodes

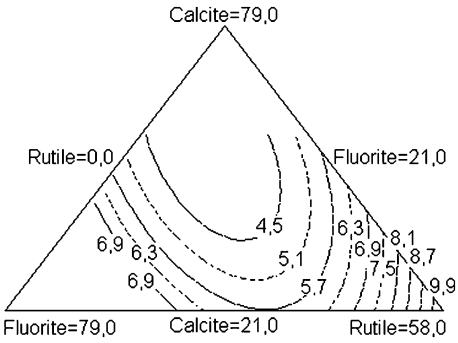

Fig. 15 Short-circuit duration (ms) at 120 A (only tsc ≥ 2 ms) as a function of calcite, fluorite, and rutile contents for the CIS-F electrodes

fusion rate values reached by CIS-C and CIS-F electrodes are very similar, not explaining by itself the higher short-circuiting frequencies for thinner grain filling (CIS-F). There is a slight tendency for CIS-F presenting smaller drops (lighter drops, as seen in Table 3). And, as seen in Fig. 11, the smaller the drops are the higher is the frequency (for a same fusion rate). In other words, this balance (smaller drops × higher frequency) justifies the same fusion rates. It seems that small size fillings make the critical size in which the transfer happens to be smaller. But, considering that the imposed voltage in the arc length controller was the same for all experiments (regardless the electrode type and batch), small variations among real arc lengths are expected. A shorter arc length would also favor higher short-circuiting frequencies. This point cannot be clarified in these experiments, since it is practically impossible to measure the real arc length in coating electrode welding.

There are several phenomena acting at the same time during metal-gas-slag reactions, which reflects on the metal transfer behavior. For instance, modifications on the metal composition due to the slag may change the drop size. According to Bracarense and Liu (Ref 27), the oxidation reactions of Si and Mn make the drop temperature to increase, justifying higher metal transfer and smaller drops. A reduction in calcite content in the slag system (in opposition to an increase in fluorite and rutile) tends to minimize gas pressure over the drop (calcite produces CO_2 in its decomposition in the arc). However, as the metal-gas-slag reactions are so complex that is difficult to predict the influence of the individual coating components on the metal transfer.

4. Conclusions

The coating composition of the electrode plays important role in the performance of a metal cored coated electrode for hardfacing. For a system based on systematic variation of calcite-fluorite-rutile, it can be deduced:

(a) The cannon-like shape of the electrode end becomes more pronounced for higher content of calcite and a lower content of fluorite. Rutile does not seem to influence this characteristic (the presence of some cannon is good for welding);
(b) The fusion and deposition rates are higher if the fluorite content in the coating is increased. The content of calcite and rutile do not seem to change the fusion behavior of the electrodes (the higher the fusion rate at a given current the more productive is the process);
(c) However, the deposition efficiency is lower when the content of fluorite increases (the higher the deposition efficiency the more economical is the process);
(d) The frequency of short-circuiting is higher for higher fluorite content in the coating (the higher the frequency the more operationally stable is the process);
(e) Concerning short-circuiting duration time, on the other hand, the most important component is calcite: the lower the calcite content the longer the short-circuiting (the shorter the short-circuiting the more operationally stable is the process);
(f) The granulometry of the alloying elements in the electrode core do not show to influence the cannon formation, fusion rate, deposition rate, and deposition efficiency. However, a coarser alloying filling presents lower short-circuiting frequencies and longer transferring time.

It can be concluded that no compound alone can improve the performance of the electrodes and a correct composition of calcite-fluorite-rutile must be found to balance the operational characteristics of the process.

Acknowledgments

The authors thank the Brazilian agency for personnel development (CAPES) and the Cuban Ministry of Higher Education (MES) for supporting this research by means of the cooperative Project CAPES/MES CUBA 15/2006. They would like to express the gratitude to the laboratorial support from Laprosolda (Center for Research and Development of Welding Processes) at the Federal University of Uberlandia, Brazil.

References

1. N.M.R. De Rissone, J.P. Farias, I. De Souza Bott, and E.S. Surian, ANS/AWS A5.1-91 E6013 Rutile Electrodes: The Effect of Calcite, *Welding Journal*, 2002, **7**, p 113s–124s
2. N.M.R. De Rissone, I.S. De Bott, J.C.F. Jorge, P. Corvalàn, and E. Surian, ANS/AWS A5.1-91 E6013 Rutile Electrodes: The Effect of Wollastonite, *Welding J.*, 1997, **76**(11), p 498s–507s
3. J.P. Farias, A.M. Quites, and E.S. Surian, The Effect of Magnesium Content on the Arc Stability of SMAW E7016-C2L/8016-C2 Covered Electrodes, *Welding J.*, 1997, **76**(6), p 245s–250s
4. J.P. Farias, A. Scotti, P.S. De, S. Bálsamo, and E.S. Surian, The Effect of Wallastonite on Operational Characteristics of AWS E6013 Electrodes, *J. Braz. Soc. Mech. Sci. Eng.*, 2004, **26**(3), p 317–322
5. Y.A. Mazel, Development of High-productivity High-alloyed Electrodes, *Weld. Int.*, 2006, **11**, p 913–917
6. V.V. Sulima and M.I. Kucherova, Ensuring the Stable Level of the Quality of Welding Electrodes, *Avt. Svarka*, 2002, **11**, p 38–41
7. I.N. Vornovitsky, N.V. Zakharova, O.V. Shishkova, A.A. Vilisov, and A.V. Zinchenko, Technological Peculiarities of High-Alloy Steel Welding by Electrodes with Rutile Coating, *Paton Weld. J.*, 2005, **2**, p 46–47
8. I.N. Vornovitsky, B.V. Semendyaev, and M.I. Kucherova, Regulating Splashing of Electrode Metal in Manual Arc Welding, *Weld. Int.*, 2007, **2**, p 157–159
9. I.R. Yavdoshchin, N.V. Skorina, A.E. Marchenko, D.Y. Vakolyuk, and A.P. Paltsevich, New Electrodes for Welding of Carbon and Low-Alloyed Steels, *Paton Weld. J.*, 2005, **3**, p 36–37
10. A.V. Yarovchuk, Effect of Ferrochrome Content on the Oxidation-reduction Processes in Welding Slags Based on Titanium Dioxide, *Weld. Int.*, 2005, **8**, p 651–656
11. I.N. Vornovitskii and I.M. Vagarov, High Productivity Electrodes for Manual Arc Welding, *Mashgiz*, 1968, **6**, p 7–10
12. I.K. Pokhodnya, V.D. Makarenko, V.N. Gorpenyuk, V. Ponomarev, O.G. Kasatkin, L.A. Taraborkin, and S.S. Milichenko, Research into the Special Features of Metal Transfer and Arc Running Stability in Welding Using Basic-Coated Electrodes. *Abt. Svarka (Automatic Weld.)*, 1984, **4**, p 39–42
13. V.V. Semendyaev, Introduction of the Quality Control System at The Elektrode Zavod Company a New Stage of Development of the Plant, *Svarshik*, 1998, **3**, p 26–29
14. E.S. Surian, ANSI/AWS E7024 SMAW Electrode: The Effect of Coating Magnesium Additions, Part 1: On The Operational Behaviour, Diffusible Hydrogen and All-Weld-Metal Mechanical Properties and Microstructure, *Weld. J.*, 1997, **76**(10), p 400–411
15. A.V. Yarovchuk, Special Features of Using Slightly Enriched Ilmenite Concentrate in the Coating of Welding Electrodes for General Applications, *Avt. Svarka*, 1997, **11**, p 46–56
16. A. Scotti, A. Quites, Y. Kobayashi, and J.P. Farias, Característica dinâmica de eletrodos revestidos (Dynamic Characteristic of Coated Electrodes). *Metalurgia*, 1984, **336**(41), p 619–622, Nov, ABM, Brazil (in Portuguese)
17. A. Cruz-Crespo, A. Scotti, and M.R. Perez, Operacional Behaviour Assesment of Coated Tubular Electrodes for SMAW Hardfacing, *J. Mater. Process. Technol.*, 2008, **199**, p 265–273 (ISSN: 0924-0136)
18. A. Cruz-Crespo, L. Perdomo Gonzalez, M.R. Pérez, R. Fernandez, and T.M. Ortiz, *Obtención de un fundente aglomerado aleado y un electrodo tubular revestido con el empleo de FeCrMn y escoria de la reducción carbotérmica de minerales* (*Agglomerated Alloyed Flux and a Metal Cored Coated Electrodes Productions Employing FeCrMn and Slag of Carbothermic Reduction of Minerals*), Congresso Brasileiro de Soldagem, ABS, Belo Horizonte, Brazil, Oct., 2006 (in Spanish)
19. H.G. Da Silva, "Desenvolvimento de Eletrodo Tubular para Soldagem Manual ao Arco Elétrico (Development of a Tubular Electrode for Manual Arc Welding)," Dissertação de Mestrado (MSc thesis), Universidade Federal de Rio Grande do Sul, Porto Alegre, Brazil, 2001, 100 p (in Portuguese)
20. M.R. Perez, "Electrodos tubular revestidos para el Relleno Superficial de Centralizadores, Estabilizadores y Piezas Sometidas a Condiciones de Desgaste Similares (Metal Cored Coated Electrodes for Hardfacing of Centralizers, Stabilizers and parts with Similar Wearing)," Disertación de Tesis Doctoral (PhD Thesis), UCLV, Santa Clara, 1992 (in Spanish)
21. S. Aknazarova and I. Kafarov, *Experimental Optimization in Chemistry and Chemical Engineering*, MIR, Moscow, 1982, p 471 (in Russian)
22. A. Cruz-Crespo, R. Quintana-Poncho, L. Perdomo Gonzalez, C.R. Gómez-Pérez, L.L. García-Sánchez, G. Ejiménez-Vielsa, and A. Cores-Sánchez, Carbothermic Reduction of Pirolusite to Obtain Carbon-Bearing Ferromanganese and Slag Suited to the Development of Welding Materials, *Weld. Int.*, 2005, **19**(7), p 544–551
23. A. Cruz-Crespo, R. Quintana-Poncho, L. Perdomo Gonzalez, L.L. García-Sánchez, C.R. Gómez-Pérez, E.D. Cedre, T.O. Mendez, and J.A. Pozol, Obtaining a Submerged arc Welding Flux of the MnO-SiO_2-CaO-Al_2O_3-CaF_2 System by Fusion, *Weld. Int.*, 2007, **21**(7), p 502–511
24. M.S. Souza and A. Scotti, Caracterização Computadorizada de Defeitos de Fabricação de Eletrodos Revestidos (Computerized Characterization of Defects from Coated Electrodes Manufacturing), *XXII Encontro Nacional de Tecnologia da Soldagem*, Blumenau, SC, Jul, ABS, 1996, p 133-143 (in Portuguese)
25. V. Podgayetskii and G. Kuzmenko, *Theory of Slags*. Naukoma Dumka, Kiev, 1998, 255 p (in Ucranian)
26. S. Brandi, C. Taniguchi, and S. Liu, Analysis of Metal Transfer in Shielded Metal Arc Welding, *Weld. J.*, 1991, **10**, p 261–270
27. A.Q. Bracarense and S. Liu, Chemical Composition Variation in Shielded Metal Arc Welds, *Weld. J.*, 1993, **12**, p 529–536